3rd URSI AT-AP-RASC, Gran Canaria, 29 May – 3 June 2022

The Angular Distribution of Chorus Waves Near Plasmaspheric Plumes

David P. Hartley*(1), Lunjin Chen (2), Ivar W. Christopher (1), Craig A. Kletzing (1),
Ondrej Santolik (3,4), Wen Li (5), and Run Shi (6)
(1) University of Iowa, Iowa City, IA, USA; email: david-hartley@uiowa.edu
(2) University of Texas at Dallas, Richardson, TX USA
(3) Institute of Atmospheric Physics, Prague, Czech Republic
(4) Charles University, Prague, Czech Republic
(5) Boston University, Boston, MA, USA
(6) Tongji University, Shanghai, China

Abstract

Plasmaspheric plumes have recently been identified as an important access region for chorus waves to enter the plasmasphere where they may subsequently be a source of plasmaspheric hiss. Here, for the first time, chorus wave properties are investigated and parameterized as a function of distance from the plume boundary. Both case study events and statistical analyses indicate that the polar wave vector angle, θ_k, of chorus waves becomes more oblique near the edge of the plume. Occurrence rates of $\theta_k > 35°$ on the plume boundary are a factor of two, or greater, than those observed further away from the plume. This increase in θ_k is evident on both the Eastward and Westward plume edges. Generally speaking, the distribution of the azimuthal wave vector angle, ϕ_k, is symmetric about the anti-Earthwards direction. However, near the Eastward plume boundary, an Eastwards skew of ϕ_k is observed. This result has important implications for modelling the propagation of chorus waves into the plasmasphere, as well as for quantifying wave-particle interactions in the near-plume region.

1. Introduction

Plasmaspheric hiss waves are one of many waves which act to drive particle dynamics in the inner magnetosphere [1], yet the origin of these waves remains somewhat of an open question. One potential source mechanism is the propagation of chorus waves into the plasmasphere, where they can provide an 'embryonic' source for hiss waves [2,3,4].

Van Allen Probes observations have been used to evaluate the angular distribution of chorus, revealing a distribution that is peaked in the anti-Earthward direction, with very few occurrences where the wave vector is oriented azimuthally Earthward [5]. However, ray tracing efforts have established that in the general case, for chorus waves to propagate into the plasmasphere, the wave vector must be oblique with respect to the background magnetic field, and oriented approximately Earthward [6,7,8,9,10]. An interesting exception is found when the chorus source is located near a plasmaspheric plume. From source regions on the edge of plumes it has been shown that the range of wave normal angles that can propagate into the plasmasphere greatly expands, and in some cases includes field-aligned waves [5,11].

This work directly identifies plasmaspheric plumes as playing an important role in the chorus to hiss mechanism. As such, direct investigation of chorus waves in the vicinity of plasmaspheric plumes is crucial to determining the coupling mechanism between chorus and hiss. This study is the first to directly evaluated the variation of chorus wave properties in the vicinity of plumes.

2. Plume and Chorus Identification

Density enhancements have been manually identified in the Van Allen Probes dataset using observations of the plasma density inferred from the upper hybrid line [12], HFR wave observations of the electric field, and WFR wave observations or both the electric and magnetic field [13]. Any density enhancements that exceed 0.2 Earth radii in either the radial or azimuthal direction are considered to be plasmaspheric plumes for the purposes of this analysis.

Across the entire Van Allen Probes mission from 2012 to 2019, 1,740 plumes have been identified using data from both spacecraft. The spatial distribution of plumes identified in this manner as a function of L shell and magnetic local time is consistent with previous studies of plasmaspheric plumes [14,15,16].

In a similar fashion to previous studies [17,18,19,20], wave observations near plasmaspheric plume density structures are categorized as chorus if they; (i) exceed a wave power threshold of 10^{-9} nT^2/Hz or 5 times the instrument background levels, whichever is higher (ii) exceed a planarity [21] threshold of 0.5, (iii) exceed an ellipticity [22] threshold of 0.5, (iv) the 2D degree of coherence in the polarization plane [23] exceeds 0.5, (v) the plasma density at the time of the observation is less than $10 \times \left(\frac{6.6}{L}\right)^4$ or 30 cm^{-3}, whichever is smaller [17]. These thresholds on planarity and ellipticity ensure no more than 14% of the total wave power, or 25% of power with respect to the largest axis of the 3-D polarization ellipsoid, is outside of the polarization plane and that the wave normal direction determined using SVD (which assumes the presence of a plane wave) is well-defined. Additionally, it is required that the plasma density at the time of the chorus observation be a factor of at least 1.5 below the average density of the nearest plume. This limits the inclusion of data from inside any plume-adjacent density enhancements.

3. Case Study

We first consider a case study where chorus waves are observed near a plasmaspheric plume by RBSP-A on 8th August 2015. Figure 1 summarizes these observations, displaying (a) the plasma density, (b) the magnetic field wave power, B_{SUM}, (c) the polar angle of the wave vector, θ_k, and (d) the median θ_k value in the lower band chorus wave frequency range. Red dots on panels a and d indicate time intervals that meet the criteria discussed above.

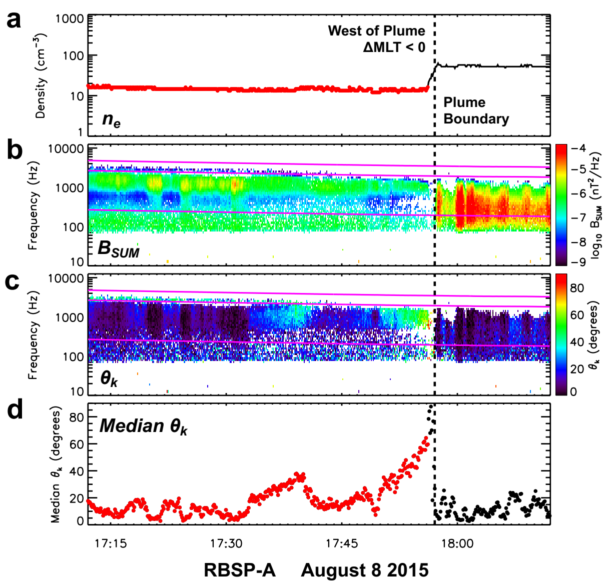

Figure 1. Case study event of chorus near a plasmaspheric plume showing (a) the plasma density, (b) magnetic field wave power, (c) wave normal angle, $\boldsymbol{\theta_k}$, and (d) median $\boldsymbol{\theta_k}$ between 0.05 and 0.50 f_{ce}. Red data indicate time periods used in the analysis.

Chorus waves are apparent outside of the plume region and all the way up to the plume boundary. For chorus far away from the plume, the waves are shown to propagate approximately parallel to the background magnetic field as indicated in panels c and d. As the spacecraft gets closer to the plume boundary, an increase in θ_k is observed. θ_k reaches a maximum value directly on the plume edge, with the median value in the lower band chorus frequency range exceeding 60° at this time.

Investigation of multiple events where chorus waves are observed near plumes reveals that this behaviour is repeatable, and occurs on both the Eastward and Westward edges of plumes. As such, this feature is investigated statistically.

4. Statistical Analysis

Chorus wave observations near all 1,740 plumes are binned as a function of separation distance from the plume boundary. This allows for us to consider the statistical behavior of the wave normal angle as a function of separation distance from the plume in MLT. Figure 2 displays the occurrence rate of oblique chorus waves as a function of distance from the plume boundary. Here, oblique waves are defined as waves where the polar wave vector angle exceeds 35°.

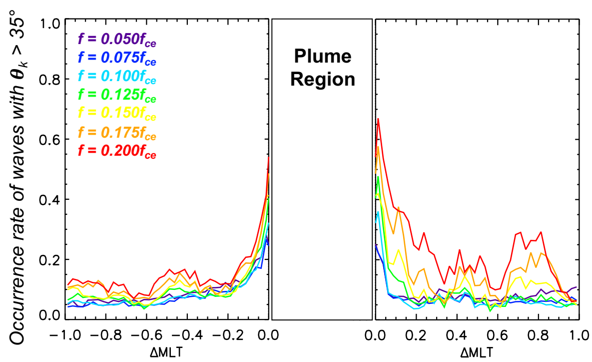

Figure 2. The occurrence rate of chorus waves with polar wave vector angles larger than 35° as a function of separation distance from the plume in MLT.

For waves far away from the plume boundary, it can be seen that for most plotted frequencies that occurrence rate of oblique waves is around 10% or less. Directly on the edge of the plume boundary however, within $|\Delta MLT| <$ 0.20, a sharp increase is observed in the occurrence rates of oblique waves. This feature occurs on both the Westward and Eastward plume edges. The maximum occurrence rate of oblique waves is observed directly on the plume boundary, where observations indicate that occurrences of oblique waves are a factor of two, or greater, than those observed further away from the plume. One possible reason for the increase in chorus wave obliquity on the plume boundary is that as the waves propagate from the low-density plasmatrough region, and begin to interact with the higher density plume, they refract. This refraction towards the higher density plume region causes an increase in the wave normal angle.

So far, only the polar wave vector angle has been considered. However, we can also investigate the azimuthal wave vector angle, ϕ_k, which is defined here as the angle of the wave vector with respect to the anti-Earthwards direction. We only consider observations of ϕ_k for time intervals when $\theta_k > 30°$ as this provides a well-defined azimuthal direction. Figure 3 shows probability distribution functions (PDFs) of ϕ_k for data (a) West of the plume, and (b) East of the plume. Different colors indicate different distances from the plume in MLT, with closest to the plume in black, to furthest away in red.

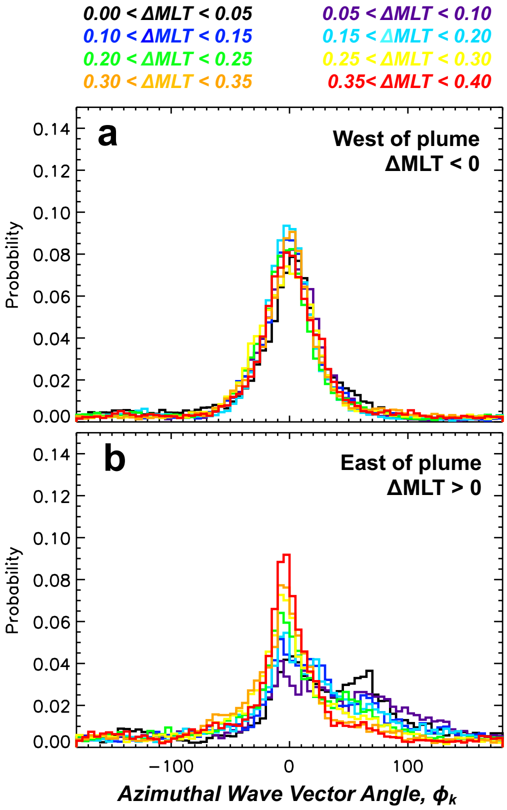

Figure 3. Probability distribution functions of the azimuthal wave vector angle for different separation distances from the (a) Westward, and (b) Eastward plume boundaries in MLT.

For observations West of the plume, all MLTs have PDFs of ϕ_k that are peaked at, and symmetric about, the anti-Earthward direction. This result is consistent with previous results [5] where it was reported that the wave vector was oriented with a component in the anti-Earthward direction for 85% of chorus wave occurrences. For observations East of the plume and separation distances greater than 0.2 MLT it is a similar picture, with PDFs peaked around the anti-Earthward direction. However, closer to the plume boundary, an asymmetry becomes apparent in the PDF of ϕ_k. This is shown in Figure 3b with PDFs for small ΔMLT values being skewed with fewer observations of $\phi_k < 0°$ and more observations of $\phi_k > 0°$. This indicates a preferentially Eastwards shift in the orientation of the wave vector on the Eastward edge of the plume. One possible explanation for this feature is that chorus waves West of the plume refract towards the plume, either propagate through or jump over the plume, and are observed on the Eastwards edge. Propagation of this type has been previously reported, but extensive ray tracing simulations are planned to thoroughly test this hypothesis.

5. Conclusions

The angular distribution of chorus waves near plasmaspheric plumes has been analyzed both for individual case study events and investigated statistically. For a case study event it has been shown that the polar wave vector angle, θ_k, of chorus waves becomes increasingly oblique near a plasmaspheric plume. The maximum obliquity is observed directly on the plume edge. A statistical analysis of 1,740 plume events identified in the Van Allen Probes dataset reveals that this increase in θ_k is apparent on both the Eastward and Westward plume boundaries. For observations within 0.2 MLT of the plume boundary, the occurrence rate of chorus propagating with $\theta_k > 35°$ is a factor of two, or greater, than that observed at larger separation distances from the plume. The azimuthal wave vector angle ϕ_k has also been analyzed to uncover differences between the Eastward and Westward plume boundary. The distribution of ϕ_k near the Westward boundary is observed to be symmetric about a central peak located in the anti-Earthward direction. On the Eastward boundary, for small separation distances from the plume, a skew in ϕ_k is observed in the Eastward direction. These features are likely attributed to propagation affects, with extensive ray tracing simulations planned in order to confirm this hypothesis. These results are the first to directly parameterize chorus observations by separation distance from the density gradients associated with plasmaspheric plumes, and provide new insight into how waves propagate in this region. These results can be tested against ray tracing simulations in order to obtain a greater understanding of the role that plumes may play in the chorus-to-hiss mechanism. These results are also important for accurate quantification of wave-particle interactions in the near-plume region, which are dependent on the angle of propagation.

6. Acknowledgements

This material is based upon work supported by the National Aeronautics and Space Administration under Grant No. 80NSSC20K1324 issued through the Heliophysics Supporting Research Program.

References

[1] Thorne, R. M. (2010), Radiation belt dynamics: The importance of wave-particle interactions, Geophys. Res. Lett., 37, L22107, doi:10.1029/2010GL044990.

[2] Bortnik, J., et al., (2009), An Observation Linking the Origin of Plasmaspheric Hiss to Discrete Chorus Emissions, Science. 2009 May 8, 324 (5928):775-8. doi:10.1126/science.1171273.

[3] Wang, C., et al., (2011), The relations between magnetospheric chorus and hiss inside and outside the plasmasphere boundary layer: Cluster

observation, J. Geophys. Res., 116, A07221, doi: 10.1029/2010JA016240.

[4] Li, W., et al., (2015), First evidence for chorus at a large geocentric distance as a source of plasmaspheric hiss: Coordinated THEMIS and Van Allen Probes observation, Geophys. Res. Lett., 42, 241-248, doi:10.1002/2014GL062832.

[5] Hartley, D. P., et al., (2019). Van Allen Probes observations of chorus wave vector orientations: Implications for the chorus-to-hiss mechanism. Geophysical Research Letters, 46, 2337-2346. https://doi.org/10.1029/2019GL082111.

[6] Chum, J. and O. Santolik, Propagation of whistler-mode chorus to low altitudes: divergent ray trajectories and ground accessibility, Annales Geophysicae, 23, 3727-3738, 2005.

[7] Bortnik, J., et al., (2008), The unexpected origin of plasmaspheric hiss from discrete chorus emissions, Nature. 3/6/2008, Vol. 452 Issue 7183, p62-66, DOI:10.1038/nature06741

[8] Bortnik, J., et al., (2011a), Modeling the evolution of chorus waves into plasmaspheric hiss, J. Geophys. Res., 116, A08221, doi:10.1029/2011JA016499.

[9] Bortnik, J., et al., (2011b), Modeling the wave power distribution and characteristics of plasmaspheric hiss, J. Geophys. Res., 116, A12209, doi:10.1029/2011JA016862.

[10] Hartley, D. P., et al., (2018). Statistical properties of plasmaspheric hiss from Van Allen Probes observations. Journal of Geophysical Research: Space Physics, 123, 2605-2619. doi.org/10.1002/2017JA024593

[11] Chen, L., et al., (2009), Three-dimensional ray tracing of VLF waves in a magnetospheric environment containing a plasmaspheric plume, Geophys. Res. Lett., 36, L22101, doi:10.1029/2009GL040451.

[12] Kurth, W. S., et al., (2015), Electron densities inferred from plasma wave spectra obtained by the Waves instrument on Van Allen Probes. J. Geophys. Res. Space Physics, 120: 904-914. doi:10.1002/2014JA020857.

[13] Kletzing, C. A., et al., (2013) The Electric and Magnetic Field Instrument Suite and Integrated Science (EMFISIS) on RBSP, Space Science Reviews, doi:10.1007/s11214-013-9993-6.

[14] Darrouzet, F., et al., (2008), Statistical analysis of plasmaspheric plumes with Cluster/WHISPER observations, Ann. Geophys., 26(8), 2403-2417.

[15] Usanova, M. E., et al., (2013), Statistical analysis of EMIC waves in plasmaspheric plumes from Cluster observations, J. Geophys. Res. Space Physics, 118, 4946-4951, doi:10.1002/jgra.50464.

[16] Kim, K.-C., and Shprits, Y. (2019). Statistical analysis of hiss waves in plasmaspheric plumes using Van Allen Probe observations. Journal of Geophysical Research: Space Physics, 124, 1904-1915. https://doi.org/10.1029/2018JA026458.

[17] Li, W., et al., (2014), Evidence of stronger pitch angle scattering loss caused by oblique whistler-mode waves as compared with quasi-parallel waves, Geophys. Res. Lett., 41, 6063-6070, doi:10.1002/2014GL061260.

[18] Hartley, D. P., et al., (2015), Applying the cold plasma dispersion relation to whistler mode chorus waves: EMFISIS wave measurements from the Van Allen Probes. J. Geophys. Res. Space Physics, 120: 1144-1152. doi: 10.1002/2014JA020808.

[19] Hartley, D. P., et al., (2016), Using the cold plasma dispersion relation and whistler mode waves to quantify the antenna sheath impedance of the Van Allen Probes EFW instrument, J. Geophys. Res. Space Physics, 121, doi:10.1002/2016JA022501.

[20] Bingham, S. T., et al. (2018). The outer radiation belt response to the storm time development of seed electrons and chorus wave activity during CME and CIR driven storms. Journal of Geophysical Research: Space Physics, 123, 10,139-10,157. https://doi.org/10.1029/2018JA025963.

[21] Santolik, O., et al., (2003), Singular value decomposition methods for wave propagation analysis, Radio Sci., 38, 1010, doi:10.1029/2000RS002523, 1.

[22] Santolik, O., et al., (2002), Magnetic component of narrowband ion cyclotron waves in the auroral zone, J. Geophys. Res., 107(A12), 1444, doi:10.1029/2001JA000146.

[23] Santolik, O., and Gurnett, D. A., (2002) Propagation of auroral hiss at high altitudes, Geophys. Res. Lett., 29 10, doi:10.1029/2001GL013666.